Penerbit Akademia Baru

Journal of Advanced Research in Micro and Nano Engineering

Journal homepage:
https://www.akademiabaru.com/submit/index.php/armne/index
ISSN: 2756-8210

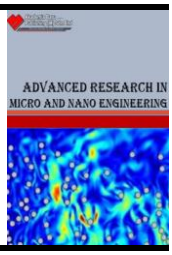

Curtailing of Torque Ripples in Switched Reluctance Motor using Nano Soft Ferrite Rotor

Kudupudi Nagesh[1], D. Lenine[2,*], P. Sujatha[1]

[1] Department of Electrical & Electronics Engineering, JNTU College of Engineering, Anantapur, Andhra Pradesh 515002, India
[2] Department of Electrical & Electronics Engineering, Rajeev Gandhi Memorial College of Engineering and Technology, Nandyala, Andhra Pradesh 518501, India

ARTICLE INFO

Article history:
Received 22 January 2024
Received in revised form 21 February 2024
Accepted 26 March 2024
Available online 30 April 2024

Keywords:
SRM; torque ripple; ferrite rotor; solution-gel auto method

ABSTRACT

Switched Reluctance motors (SRM) enthralled many researchers due to their coherent structure and sturdy design switched reluctance motors are, robust, reliable, fault tolerated, efficient, and maximum temperature resistant when compared to other conventional motors. The drift in the power electronic converters enhances the usage of SRM, stator and rotor consisting of projected inward and outward poles the gap between the stator and rotor causes harmonics which cause torque ripples which are deteriorating SRM drives. In this paper, a ferrite rotor is considered which is composed by the different material like nickel, manganese, copper, ferric, and aluminium by manoeuvring combustion of solution and gel method. By availing ferrite material magnetizing and demagnetizing can be done quickly which is essential for SRM rotor.

1. Introduction

Switched Reluctance motor attaining more focus when compared to conventional motors due to its sturdy design and coherent structure the alluring attributes are robustness, highly reliable, fault tolerated, efficiency and maximum temperature resistant SRM are suffering from high torque ripples leading to high noise. The stator consists of poles outwards and the rotor consists of poles inwards, the stator is made up of a permanent magnet and the rotor is made of a solid laminations structure that does not have any windings since the structure is simple and the value of SRM became less which turned SRM supremacy based on structure of stator and rotor poles and they are differentiated by 8/6 and 6/4 [1-3]. The SRM motor consists of a stator/rotor pole 8/6 simple construction is represented in Figure 1. SRM works on the reluctance principle, its operation can be effectively improved by two methods one is by the proper mechanical design and another by considering righteous advanced controllers considering accurate amplitudes of current, voltage, turn-on and turn-off angles. SRM motor character structure has the number of stator and rotor poles are not equal, magnetic flux is not pure Sine curve, mutual inductance in phase winding is very less, and the value of torque generated is self-contained of the polarity related to stator current. The windings

* *Corresponding author.*
E-mail address: lenine.eee@gmail.com

https://doi.org/10.37934/armne.18.1.5259

inductance is so high that removal energy saved is needed restricting the maximum current to a low range. The Block diagram operation of SRM is represented in Figure 2 of the rotor is sensed by a sensor represented by angle, 'ɵ 'when ɵ=0 starting point phase A position is un aligned to midpoint of inter polar rotor-gap faces the stator pole.at this position there is no torque and the current is passing in phase A [4-7]. A torque is required to bring rotor position from unaligned to aligned where the stator and rotor pole centres coincide if the rotor position is ectopic to other side of the unaligned position, unstable equilibrium characterises the mis- aligned situation, since the rotor is in apposition of ace value of inductance when current is passing in an aligned position there is zero torque [12-18]. Here in this paper, it is mainly focused on rotor material. Conventional rotor material is generally made up of soft magnet like iron-silicon alloys, nickel-iron alloys and iron [8-12]. The coercivity is less than the position $1000Am^{-1}$.

2. Mathematical Equations of SRM

Where 'P' Phase machine, stable equilibrium is obtained when rotor position is aligned. Stator poles are represented by P1 and rotor poles are represented by P2 no. of phase's equation is given in Eq. (1) and Eq. (2)

$$\text{Phase Machine } P = P1/ (P1-P2) \tag{1}$$

$$\text{Number of pole pairs} = P1/2P \tag{2}$$

Expression for stator pitch and rotor pole pitch is given in Eq. (3) and Eq. (4)

$$\text{Stator Pitch } \Gamma s = 2\Pi/P2 \tag{3}$$

$$\text{Rotor Pitch } \Gamma r = 2\Pi/P1 \tag{4}$$

The shift change in phase is between flux linkages and stator phase and it is obtained in Eq. (5) as given below

$$\text{Phase Shift } \Theta_{PS} = (2\Pi/P2) * (1/P) \tag{5}$$

The stroke angle obtained from the difference of the stator pole pitch and rotor pole pitch is expressed in Eq. (6)

$$\text{Stroke angle } \Theta_{sa} = \Gamma s - \Gamma r \tag{6}$$

For one phase switching frequency can be written by based on Eq. (7)

$$\text{Phase Switching Frequency } P_f = P * P2 \tag{7}$$

The conventional method of using SRM sends uni-directional current signals progressively to each phase coils this signal timing and amplitude might be used to limit it. Due to its unique design and lack of magnetic excitation current and no mutual inductance in coils the back emf is produced by the change in phase excited by self-inductance. The count of stator poles and rotor poles and their physical dimensions are the number of phases in stator and, the intensity of phase current is the

timing of the phase on off affect this power and mechanical torque Due to a significant angle between the poles of the stator and rotor, the SRM can have the greatest proportion between phase of aligned & unaligned inductance.

3. Nano Soft Ferrite SRM Rotor

Cubic spine structured ferrite contains good magnetic and electrical properties related to their method of preparation, temperature and time taken for preparation. Interaction between oxygen ions and metal electrons ferrites possess ferrimagnetism the resistivity of ferro-magnetism is low when compared to ferrite. Spinal class ferrites and nickel ferrites gives good stability, saturated magnetization, high resistivity and high coercivity, stoned nickel ferrite & nickel ferrites are examined by many researchers because of their composed distinct elements. Ni-Mn ferrite material chemical formula is given by $_1Fe_{2-}xAlxO4$ $Ni_{0.7}Mn_{0.2}Cu_{0.}$ The value *x* ranges from 0, 0.05, 0.1, 0.15, 0.2, and 0.25 with respect to composition & frequency. $Ni_{0.7}Mn_{0.2}Cu_{0.1}Fe_{2-}xAlxO4$ six samples are considered in the preparation of nano ferrites by using auto sol-gel method. Interpretive agents chemicals are introduced $Ni(NO3)_{2.}6H_2O$Nitratesof Nickel greater than equal to 98%, Merck, $Mn(NO_3)_2.6H_2O$ Manganese equals to 99 percent Merck, $Cu(NO_3)_{2.}3\ H_2O$ copper equals to 99% Himedia, $Fe(NO_3)_3.9\ H_2O$ ferric equals to 99 percent Himedia, $Al(NO_3)\ 9\ H_2O$ aluminium equals to 99% Himedia) and citric acid $C_6H_8O_7$ (Merck) are used for obtaining solution for synthesis process is converted into gel by high temperature for one quadrature hours at eighty degrees Celsius the powder is manufactured and pellets are coalesce at one thousand two hundred degrees Celsius for 5 Hrs the above flow chart describes the procedure for sampling synthesis as shown in Figure 1. Himedia and Merck are the manufacturers of chemicals and reagents for research work.

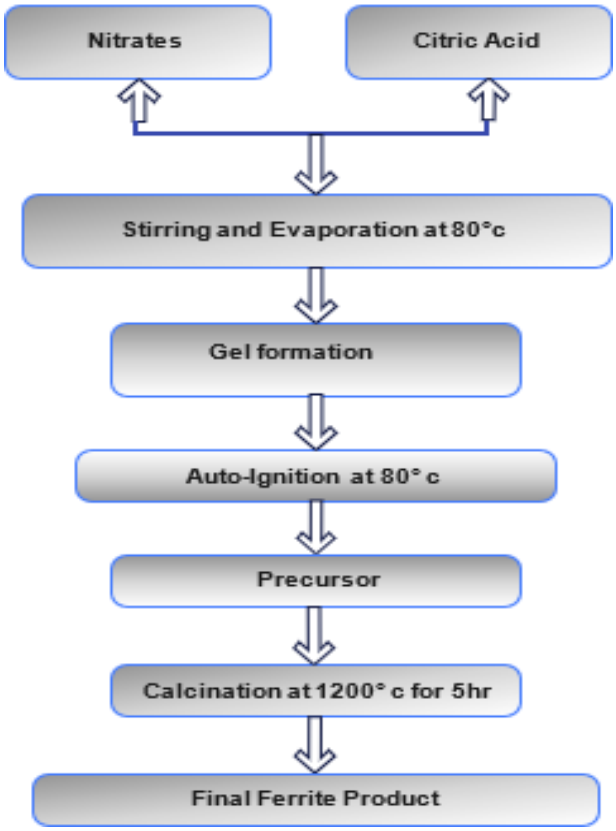

Fig. 1. Flow chart of solution-gel auto method

Where A1A2, B1B2, C1C2, D1D2, are four phases of stator which represents 8 stator poles respectively and 6 rotor poles. It is clearly shown in Figure 2.

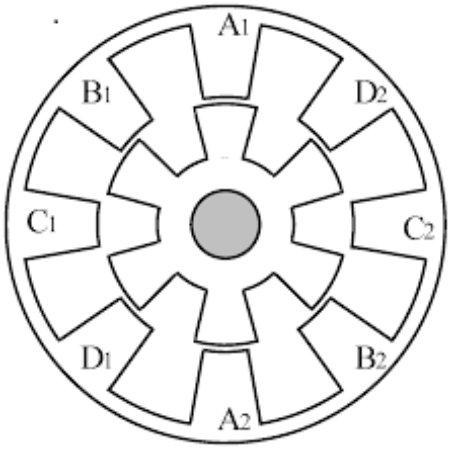

Fig. 2. 8/6 SRM structure

The block diagram of proposed system as shown in Figure 3.

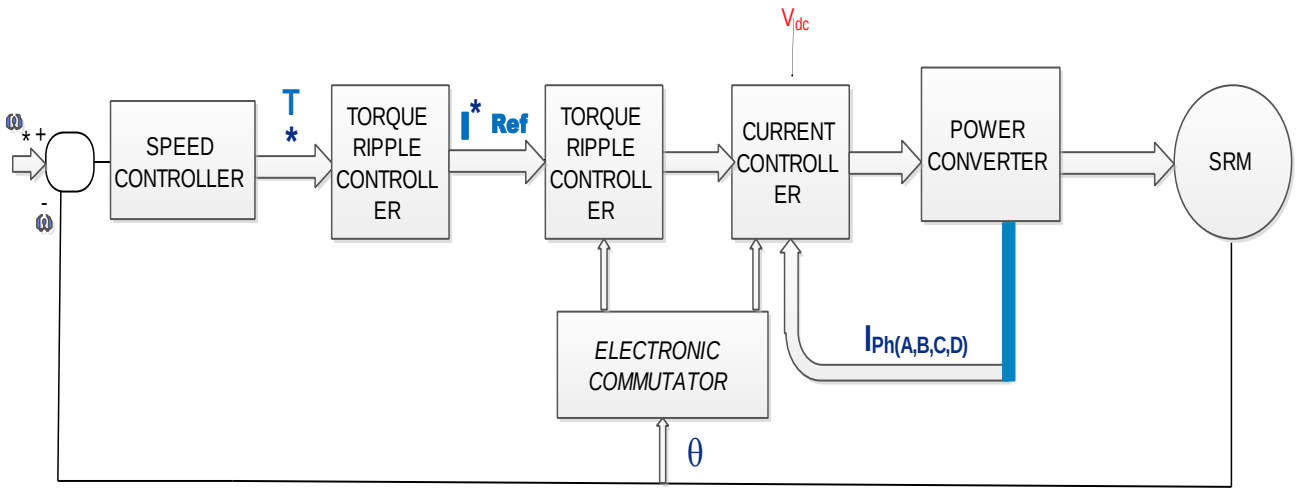

Fig. 3. Block diagram representation of SRM

4. Results and Discussion

The value x ranges from 0, 0.05, 0.1, 0.15, 0.2, and 0.25 with respect to composition and frequency synthesized nano ferrite dielectric is plotted with frequency as show in Figure 4 di-electric decreases with increase in frequency it is exponential and similar to Maxwell-Wagner space charge polarization in synchronization with Koop's phenomenon. Maxwell-Wagner explains when electric field is applied high electrical displacement of nanocomposite is resulted, and therefore enhances pristine polymers.

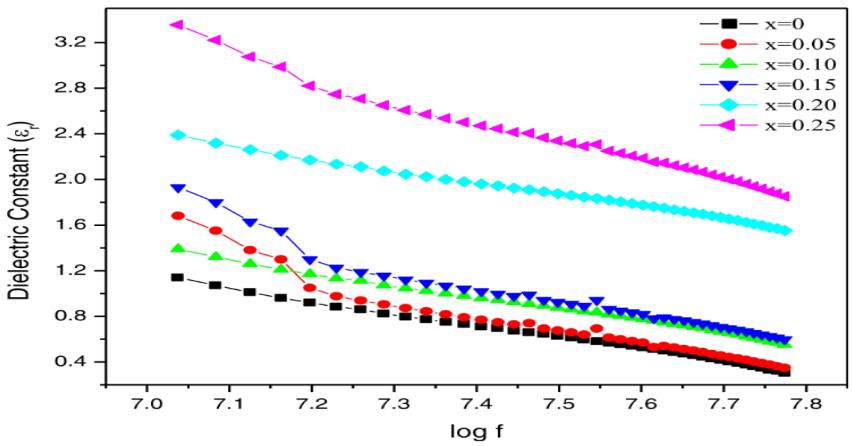

Fig. 4. $Ni_{0.7}Mn_{0.2}Cu_{0.1}Fe_{2}$-xAlxO4 the value of x ranges from 0, 0.05, 0.1, 0.15, 0.2, and 0.25 with respect to εr & frequency

The dielectric decrease is due to the electronic exchange between ferrous and ferric ions at a particular frequency. The dielectric loss tan δ is varied with frequency for every synthesized nano-ferrite $Ni_{0.7}Mn_{0.2}Cu_{0.1}Fe_{2}$-xAlxO4(x =0,0.05,0.1,0.15,0.2 and 0.25) is shown in Figure 5 di electric losses decreases with increase in frequency, the response of dielectric loss can be explained with the help of Maxwell -Wagner interfacial polarization.

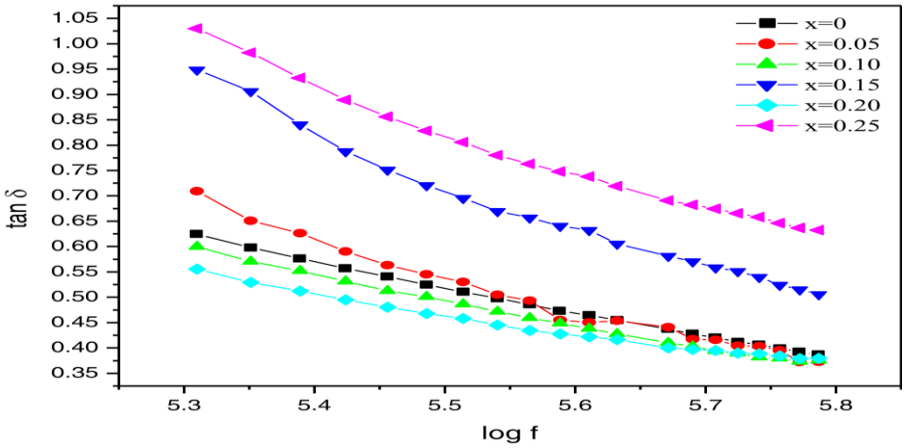

Fig. 5. $Ni_{0.7}Mn_{0.2}Cu_{0.1}Fe_{2}$-xAlxO4 the value *x* ranges from 0, 0.05, 0.1, 0.15, 0.2, and 0.25 with respect to tan δ & frequency

DC resistivity changes with frequency as shown in the Figure 6 for $Ni_{0.7}Mn_{0.2}Cu_{0.1}Fe_{2}$-xAlxO4(x =0,0.05,0.1,0.15,0.2 and 0.25) nano ferrite material decrease in the resistivity is due to large ionic radius of Fe^{3+} when compared to Al^{3+} in the ferrite current and aluminium swapping in iron. The reduction in the resistivity reduces the porosity as pores are unavailable to promoting for conduction which helps for resistivity. The resistivity decreases with porosity as the carriers on their way leads to pores.

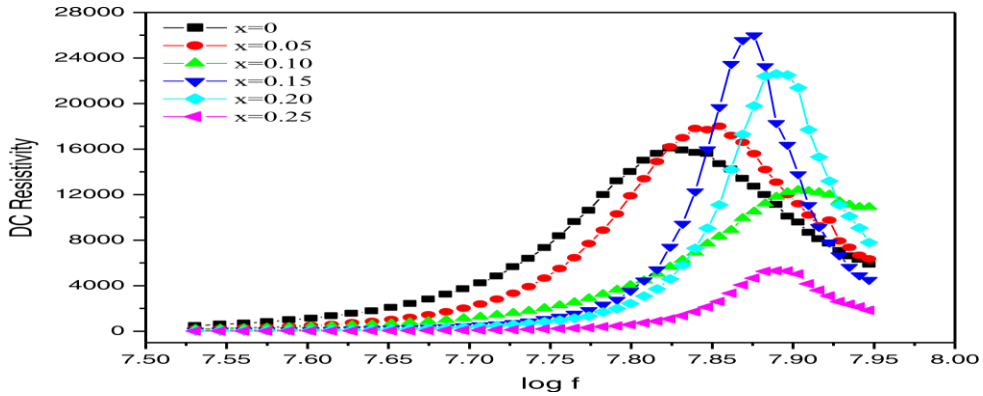

Fig. 6. Ni0.7Mn0.2Cu0.1Fe2-xAlxO4 the value x ranges from 0, 0.05, 0.1, 0.15, 0.2, and 0.25 with respect to resistivity & frequency

The magnetic behaviour when field is applied at room temperature for $Ni_{0.7}Mn_{0.2}Cu_{0.1}Fe_{2}$-xAlxO4 the value x ranges from 0, 0.05, 0.1, 0.15, 0.2, and 0.25 is shown in the Figure 7.

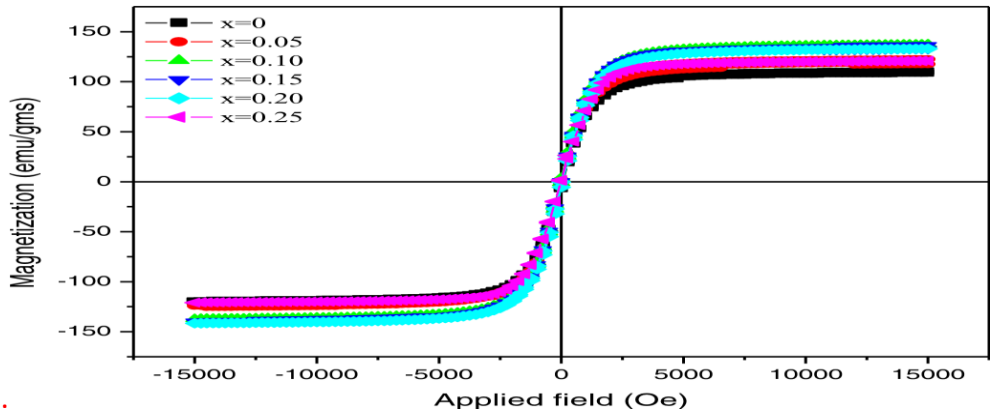

Fig. 7. M-H Loop for $Ni_{0.7}Mn_{0.2}Cu_{0.1}Fe_{2}$-xAlxO4 the value x ranges from 0, 0.05, 0.1, 0.15, 0.2, and 0.25

SRM nano-ferrite rotor enhances the magnetic properties when compared to soft magnetic materials from the figure the magnetization value is stepped up with adapted magnetic field and attains the maximum position at higher magnetic field with the help of M-H plot Magnetic saturation, the magnetic moment and coercivity are obtained and tabled as below.

Table 1
Magnetic Properties

x-value	Saturation magnetization (M_g) (emu/gm)	Magnetic moment (?$_B$)	Coercivity (H_c) (Oe)	g-value
0	126.9806	2.9360	24	1.9629
0.05	107.2839	4.4694	39	2.0526
0.01	114.5964	4.7444	37	2.1140
0.15	120.6067	4.9621	29	2.0625
0.20	129.2215	5.2831	22	1.9820
0.25	135.2318	5.4939	21	1.9758

The magnetic saturation and coercivity are obtained from the M-H plot. From the above Table 1, the values of coercivity state nano crystalline nature of synthesized nano ferrites. The value of coercivity decreases with increase in aluminium concentration. The coercivity of nano ferrites rely on crystalline anisotropy constant, grain size average, lower value of coercivity results decrease in

magnetic losses. The impregnation of aluminium in iron ferrite causes magnetic saturation, magnet on number, coercively and magnetic properties drop. The rotor made of nano ferrites has higher efficiency. The declination in coercively with increase in aluminium content size of the particle and saturation magnetization continuously increases. The magnetic saturation and magnetic ruminant are greatly dependent on sintering temperature nano ferrites size greatly depending on temperature sintering from all the above properties nano ferrites materials expose super magnetic behaviours. Sintering is a heat treatment process where loose material is subjected to high temperature and pressure in order to compact it into a solid piece Figure 8 represents relation between initial permeability with frequency.

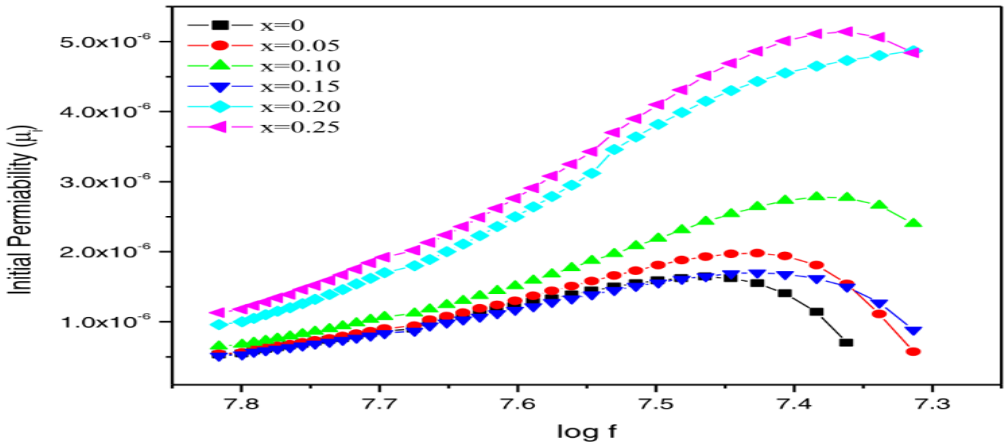

Fig. 8. Initial permeability with frequency for $Ni_{0.7}Mn_{0.2}Cu_{0.1}Fe_{2}$-xAlxO4 the value x ranges from 0, 0.05, 0.1, 0.15, 0.2, and 0.25

Magnetic properties when compared to conventional soft magnetic material the results are analysed and displayed in exhibits good the graph and tables. Nano ferrites are synthesized with the help of the auto sol-gel combustion method the material obtained from this method is used for the rotor.

5. Conclusion

SRM Nano ferrite rotor $Ni_{0.7}Mn_{0.2}Cu_{0.1}Fe_{2}$-xAlxO4 the value x ranges from 0, 0.05, 0.1, 0.15, 0.2, and 0.25 exhibits good magnetic properties when compared to conventional soft magnetic material the results are analysed and displayed in the graph and tables. Nano ferrites are synthesized with the help of the auto sol-gel combustion method the material obtained from this method issued for the rotor.

Acknowledgement
This research was not funded by any grant.

References
[1] Pushparajesh, V., B. M. Nandish, and H. B. Marulasiddappa. "Hybrid intelligent controller based torque ripple minimization in switched reluctance motor drive." *Bulletin of Electrical Engineering and Informatics* 10, no. 3 (2021): 1193-1203. https://doi.org/10.11591/eei.v10i3.3039

[2] Keerthana, C., and M. Sundaram. "State of art of control techniques adopted for torque ripple minimization in switched reluctance motor drives." In *2020 4th International Conference on Trends in Electronics and Informatics (ICOEI)(48184)*, pp. 105-110. IEEE, 2020. https://doi.org/10.1109/ICOEI48184.2020.9143012

[3] Rana, Ashwani Kumar, and AV Ravi Teja. "A mathematical torque ripple minimization technique based on a nonlinear modulating factor for switched reluctance motor drives." *IEEE Transactions on Industrial Electronics* 69, no. 2 (2021): 1356-1366. https://doi.org/10.1109/TIE.2021.3063871

[4] Reddy, M. Madhusudhan, P. Srinivasa Varma, and D. Lenine. "Central Force Optimization Technique based Harmonic Mitigation in Shunt Active Power Filters." *International Journal of Intelligent Systems and Applications in Engineering* 10, no. 4 (2022): 527-533.

[5] Zhang, Zhiwei, and Libing Zhou. "Design and rotor geometry analysis of permanent magnet–assisted synchronous reluctance machines using ferrite magnet." *Journal of Electrical Engineering* 66, no. 6 (2015): 311-316. https://doi.org/10.2478/jee-2015-0051

[6] Priyanka, G., J. Surya Kumari, D. Lenine, P. Srinivasa Varma, S. Sneha Madhuri, and V. Chandu. "MATLAB-Simulink environment based power quality improvement in photovoltaic system using multilevel inverter." (2023). https://doi.org/10.20998/2074-272X.2023.2.07

[7] Wcislik, Mirosaw, and Karol Suchenia. "Analysis of the influence of material parameters on efficiency of switched reluctance motor." In *2018 Conference on Electrotechnology: Processes, Models, Control and Computer Science (EPMCCS)*, pp. 1-5. IEEE, 2018. https://doi.org/10.1109/EPMCCS.2018.8596512

[8] Nagesh, K., D. Lenine, and P. Sujatha. "Design and Development of Sensorless Vector Control of Switched Reluctance Motor using Fuzzy Logic Controller." (2020).

[9] Rajkumar, S., K. Sedhuraman, and D. Murugadhan. "Thermal analysis and torque ripple minimization in switched reluctance motor with Nickel-Ferrite material." In *2018 ieee international conference on system, computation, automation and networking (icscan)*, pp. 1-4. IEEE, 2018. https://doi.org/10.1109/ICSCAN.2018.8541200

[10] Boldea, Ion, Lucian N. Tutelea, Leila Parsa, and David Dorrell. "Automotive electric propulsion systems with reduced or no permanent magnets: An overview." *IEEE Transactions on Industrial Electronics* 61, no. 10 (2014): 5696-5711. https://doi.org/10.1109/TIE.2014.2301754

[11] Shimomura, Shoji, and Takatoshi Sunaga. "Design of integrated radial and dual axial-flux ferrite magnet synchronous machine." In *2016 IEEE Energy Conversion Congress and Exposition (ECCE)*, pp. 1-6. IEEE, 2016. https://doi.org/10.1109/ECCE.2016.7855026

[12] Zhao, Wenliang, Dezhi Chen, Thomas A. Lipo, and Byung-Il Kwon. "Performance improvement of ferrite-assisted synchronous reluctance machines using asymmetrical rotor configurations." *IEEE Transactions on magnetics* 51, no. 11 (2015): 1-4. https://doi.org/10.1109/TMAG.2015.2436414

[13] Mohan, P. Rama, K. Niteesh Kumar, G. Bala Subbarayudu, A. Suresh Kumar, and D. Lenine. "Novel scalar PWM techniques for vector control based induction motor drives to reduce common mode voltage." *J Mech Cont & Math Sci, Special Issue* 3 (2019): 52-67.

[14] Zhang, Zhiwei. "Design and experimental verification of low cost ferrite PM-assisted synchronous reluctance motor." In *2020 IEEE Transportation Electrification Conference & Expo (ITEC)*, pp. 327-334. IEEE, 2020. https://doi.org/10.1109/ITEC48692.2020.9161455

[15] Pošković, Emir, Luca Ferraris, and Nicola Bianchi. "Two approaches in the use of ferrites in assisted reluctance machines." In *2020 International Symposium on Power Electronics, Electrical Drives, Automation and Motion (SPEEDAM)*, pp. 670-675. IEEE, 2020. https://doi.org/10.1109/SPEEDAM48782.2020.9161929

[16] Akiki, Paul, Maya Hage Hassan, Jean-Claude Vannier, Mohamed Bensetti, Benjamin Dagusé, and Mike McClelland. "Performance comparison of a doubly-salient motor with multi-V-shape ferrite magnets." In *2016 International Symposium on Power Electronics, Electrical Drives, Automation and Motion (SPEEDAM)*, pp. 205-212. IEEE, 2016. https://doi.org/10.1109/SPEEDAM.2016.7525826

[17] Sutka, Andris, and Gundars Mezinskis. "Sol-gel auto-combustion synthesis of spinel-type ferrite nanomaterials." *Frontiers of Materials Science* 6 (2012): 128-141. https://doi.org/10.1007/s11706-012-0167-3

[18] Hasan, Sarwar, and Bruska Azhdar. "Synthesis of Nickel-Zinc Ferrite Nanoparticles by the Sol-Gel Auto-Combustion Method: Study of Crystal Structural, Cation Distribution, and Magnetic Properties." *Advances in Condensed Matter Physics* 2022 (2022). https://doi.org/10.1155/2022/4603855